

Altering the Substrate Specificity and Enantioselectivity of Phenylacetone Monooxygenase by Structure-Inspired Enzyme Redesign

Daniel E. Torres Pazmiño,^a Radka Snajdrova,^b Daniela V. Rial,^b Marko D. Mihovilovic,^{b,*} and Marco W. Fraaije^{a,*}

^a University of Groningen, Department of Chemistry, Biotechnology Group, Nijenborgh 4, 9747 AG Groningen, The Netherlands

Fax: (+31)-50-363-4165; e-mail: m.w.fraaije@rug.nl

^b Vienna University of Technology, Institute of Applied Synthetic Chemistry, Getreidemarkt 9/163-OC, 1060 Vienna, Austria

Fax: (+43)-1-58801-15499; e-mail: mmihovil@pop.tuwien.ac.at

Received: January 23, 2007

Abstract: Of all presently available Baeyer–Villiger monooxygenases, phenylacetone monooxygenase (PAMO) is the only representative for which a structure has been determined. While it is an attractive biocatalyst because of its thermostability, it is only active with a limited number of substrates. By means of a comparison of the PAMO structure and a modeled structure of the sequence-related cyclopentanone monooxygenase, several active-site residues were selected for a mutagenesis study in order to alter the substrate specificity. The M446G PAMO mutant was found to be active with a number of aromatic ketones, amines and sulfides for which wild-

type PAMO shows no activity. An interesting finding was that the mutant is able to convert indole into indigo blue: a reaction that has never been reported before for a Baeyer–Villiger monooxygenase. In addition to an altered substrate specificity, the enantioselectivity towards several sulfides was dramatically improved. This newly designed Baeyer–Villiger monooxygenase extends the scope of oxidation reactions feasible with these atypical monooxygenases.

Keywords: asymmetric catalysis; Baeyer–Villiger monooxygenase; biotransformations; enzyme redesign; indigo blue; sulfoxidation

Introduction

The number of processes in which biocatalysts are involved is steadily growing. Biocatalysts are frequently exploited for their exquisite regio- or enantioselectivity for the synthesis of pharmaceutical building blocks while they are also increasingly being explored for application in the synthesis of low-value chemicals. Alongside with this increase in biocatalyst implementation, more and more biocatalysts have become available. Due to the efforts of biocatalyst discovery and redesign in the last decade, a huge number of novel enzymes have emerged on the market. However, while the arsenal of hydrolytic enzymes is quite extensive nowadays, the number of applicable oxidative biocatalysts is lagging behind. To satisfy the growing demand for novel oxidative biocatalysts, we focus on the discovery and redesign of such enzymes.

An interesting class of oxidative biocatalysts is represented by the Baeyer–Villiger monooxygenases (BVMOs).^[1] Products obtained by BVMO-mediated

biooxidations are of great value in organic synthesis and the pharmaceutical chemistry.^[2] While only a few BVMOs were known and have been explored for biocatalytic purposes since the beginning of the 1970s, in recent years several other BVMOs have been reported in literature.^[3] Biocatalytic studies on these BVMOs have revealed that these biocatalysts do not only catalyze Baeyer–Villiger oxidations but also are able to oxidize sulfides and other heteroatom-containing compounds. Except for this promiscuity in reactivity, BVMOs are often very enantio-, regio- and/or chemoselective while accepting a broad range of substrates. Recently we have obtained a novel BVMO, phenylacetone monooxygenase (PAMO, EC 1.14.13.92), which offers several unique and attractive features: (1) it is thermostable and tolerant towards organic solvents,^[4] (2) it has been shown to catalyze enantioselective Baeyer–Villiger oxidations and sulfoxidations,^[5] and (3) it represents the only BVMO for which a crystal structure is available.^[6] While a number of substrates, mainly aromatic, have been

identified for phenylacetone monooxygenase from *Thermobifida fusca*, it shows poor or no activity with aliphatic compounds. This contrasts with the relaxed substrate acceptance profiles of cyclohexanone monooxygenase (CHMO, EC 1.14.13.22) from *Acinetobacter* sp. NCIMB 9871^[7] and cyclopentanone monooxygenase (CPMO, EC 1.14.13.16) from *Comamonas* sp. strain NCIMB 9872,^[8] which are the most extensively studied BVMOs.^[9] These enzymes efficiently convert a wide range of aliphatic ketones and are complementary in respect to their enantioselectivity towards several of these ketones. Unfortunately, CHMO and CPMO display a poor stability in comparison to PAMO.^[10]

While they display widely differing substrate specificities, CPMO and PAMO are closely related as they share 41% sequence identity. This level of sequence homology has allowed us to build a structural model of CPMO. Inspection of the active site of CPMO revealed that most residues located at the *re* face of the bound FAD cofactor (e.g., PAMO residues N58, D66, S196, Q200, K336, R337, F389, Y495 and W501), forming the substrate binding pocket, are identical in both enzymes. Conservation of R337 is not surprising as it is the key active site residue which assists in catalysis.^[6] Only three residues were strikingly different: Q152, L153 and M446 in PAMO align with F156, G157 and G453 in CPMO (Figure 1). The F156 and G157 residues of CPMO have recently been confirmed as hotspots in tuning enantioselectivity of CPMO.^[11]

In this paper we report the change of PAMO substrate specificity by replacing M446: the M446G PAMO mutant. In addition to an altered substrate

specificity, the active-site redesign results in improved enantioselective behavior. Furthermore, we applied a parallel screening methodology recently developed for the evaluation of whole cells biocatalyst performance and stereoselectivity, demonstrating that wild-type and M446G PAMO can be exploited using whole cells.^[12]

Results and Discussion

Cloning, Purification and Characterization of PAMO Mutants

Based on the structural differences of the (predicted) active sites of CPMO and PAMO, we prepared a single, a double and a triple mutant of PAMO by means of site-directed mutagenesis: (i) M446G, (ii) Q152F/L153G and (iii) Q152F/L153G/M446G. Overexpression and purification of these mutants (see Experimental Section) resulted in three soluble mutant proteins containing a tightly bound FAD cofactor. All mutants were tested for activity with several potential substrates (phenylacetone, cyclopentanone, cyclohexanone) by following the rate of NADPH consumption in time at 340 nm.

The double and the triple PAMO mutants were found to be inactive with these ketones as only a slow conversion of NADPH was observed with concomitant production of hydrogen peroxide. This indicates that these mutants are still able to bind NADPH and reduce the flavin cofactor, while they have lost the ability to perform oxygenation reactions. As a result they merely act as NADPH oxidase with rates of 0.06 s^{-1} for the Q152F/L153G mutant and 0.6 s^{-1} for the M446G/Q152F/L153G mutant. A similar rate (0.05 s^{-1}) of uncoupled NADPH consumption has been observed for wild-type PAMO when no substrate is present.^[3d] Although the modeled active site of CPMO appears quite similar to that of PAMO, these results indicate that the Q/L→F/G substitutions in PAMO result in an active site architecture that is not effective in proper binding and/or positioning of substrates. Improper positioning of substrates with respect to the flavin cofactor will hinder an effective nucleophilic attack of the peroxyflavin that is required for oxygenation of the substrate. A recent study has shown that the corresponding residues in CPMO can be varied to some extent thereby influencing the enantioselectivity. However, it should be noted that all reported conversions using these CPMO mutants resulted in relatively poor conversions when compared with wild-type CPMO.^[11,13] This again hints to the fact that these residues are crucial for proper catalysis.

The M446G PAMO mutant showed significant activity towards phenylacetone (**1**) while no activity was

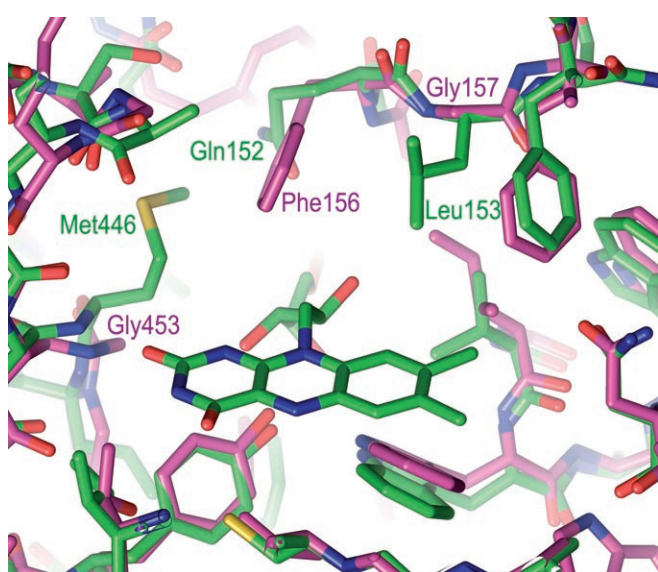


Figure 1. Representation of the active-sites of PAMO (green) and CPMO (purple).

observed with cyclopentanone and cyclohexanone. The mutant displayed an identical uncoupling rate when compared to wild-type PAMO. In the absence of a suitable substrate the mutant enzyme oxidized NADPH at a rate of 0.1 s^{-1} . A hint for an altered substrate specificity for the M446G mutant was already obtained during growth of *E. coli* cells expressing the respective enzyme. During growth of M446G PAMO-expressing cells, the culture medium turned blue suggesting that indigo blue was formed during cultivation. Indigo production has been observed in *E. coli* before when expressing other types of mono- or dioxygenases.^[14] This observation suggests that the endogenous indole (**14**), generated from tryptophan by tryptophanase in *E. coli*,^[15] is oxidized by this specific PAMO mutant and subsequently undergoes spontaneous dimerization to yield indigo blue. Thus far, no other BVMO has been found which is able to form indigo blue from indole.

Substrate Specificity and Steady-State Kinetics of M446G PAMO

Using isolated enzyme, the substrate acceptance profile of M446G PAMO was explored in comparison with the wild-type enzyme. This has revealed that, besides phenylacetone (**1**) and indole (**14**), M446G PAMO accepts a number of other organic substrates, including ketones/aldehydes, sulfides and amines. The steady-state kinetic parameters for these substrates are shown in Table 1. Compared to wild-type PAMO, the apparent affinity (K_M) of the mutant enzyme towards the physiological substrate, phenylacetone (**1**), decreased 10-fold. The activity of the mutant enzyme was found to be identical to that of wild-type PAMO: $k_{\text{cat}} = 3.0 \text{ s}^{-1}$. Using phenylacetone as substrate the thermostability of the M446G mutant was tested at 50°C . A half-life time of $55 \pm 6 \text{ h}$ was found which is comparable to that of wild-type PAMO.^[3d] This shows that the mutation does not affect the thermostability. The catalytic efficiency towards several known PAMO substrates **2**, **5**, and **9** was also not affected by the mutation. Interestingly, while some substrates accepted by wild-type PAMO were not accepted by M446G PAMO (4-hydroxyacetophenone and *N,N*-dimethylbenzylamine), the PAMO mutant showed activity towards several aromatic substrates (**3**, **11**, **13** and **14**) that are not converted by wild-type PAMO.

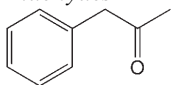
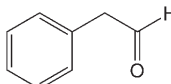
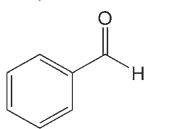
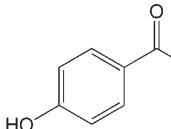
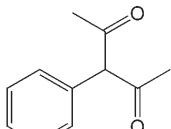
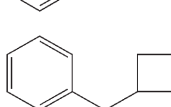
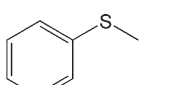
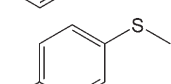
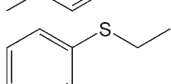
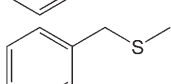
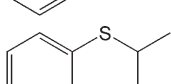
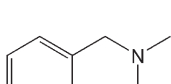
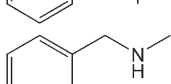
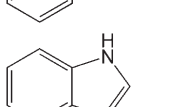
We were also able to confirm that purified M446G PAMO is capable of forming indigo blue from indole as substrate. The ability of this mutant to convert indole was unexpected as the BVMO-catalyzed production of indigo blue from indole has not been observed before. Previous studies have shown that monooxygenases are able to produce indigo upon epoxidation or hydroxylation of indole.^[14a-c] However,

BVMOs are not able to perform hydroxylations and are very poor epoxidation catalysts.^[16] We also confirmed that wild-type PAMO and M446G PAMO are unable to hydroxylate or epoxidize the indole-related compounds styrene, indene and cinnamyl alcohol. We concluded that indigo formation from indole is most likely the result of *N*-oxidation of indole, as has been previously suggested for a distantly related flavin-containing monooxygenase.^[14d] The formed indole *N*-oxide is expected to rearrange into indoxyl, which would yield indigo blue upon spontaneous dimerization. Such a rearrangement has also been observed for related *N*-oxides.^[17] To our knowledge such a synthetic route towards indigo blue has not been described before and it may offer interesting alternative routes for synthesis of indigo derivatives. In addition to indole, also another secondary amine, *N*-methylbenzylamine, was accepted by M446G PAMO while this amine is not a substrate for wild-type PAMO. In contrast, it was previously demonstrated that wild-type PAMO oxidizes the tertiary amine, *N,N*-dimethylbenzylamine,^[5] while this amine is not accepted by M446G PAMO. This indicates that the engineered mutant readily accepts secondary amines. These results show that replacing M446G has dramatic effects on the substrate acceptance profile.

Enantioselective Sulfoxidations by Purified M446G PAMO

While it has been observed in previous studies that wild-type PAMO efficiently oxidizes a wide range of aromatic sulfides (Table 1),^[5] the enzyme mediated oxidation was often not very enantioselective. As can be seen in Table 1, the M446G PAMO also readily converts a number of aromatic sulfides. In fact, one sulfide was discovered that is not accepted by wild-type enzyme while it is oxidized by the mutant. To determine the enantioselectivity of this oxidation, 2 mL reactions were performed using purified mutant enzyme in the presence of glucose 6-phosphate dehydrogenase for regeneration of NADPH. Analysis of these conversions by chiral GC showed that the M → G mutation resulted in a substantial increase in enantioselectivity of several product sulfoxides (Table 2). The enantioselectivity with thioanisole (**7**) increased from a moderate ($ee_{\text{wt}} = 41\%$) to an excellent enantioselectivity ($ee_{\text{M446G}} = 93\%$). Even more impressive results were obtained for sulfides **8** and **9** for which the wild-type enzyme displayed almost no enantioselectivity ($ee_{\text{wt}} = 6\%$) while the mutant enzyme shows an excellent enantioselectivity ($ee_{\text{M446G}} = 92$ and 95% , respectively). With all three sulfides, the corresponding (*R*)-sulfoxides were predominantly formed. In contrast, conversion of benzyl methyl sulfide (**10**) yields mainly the (*S*)-sulfoxide. The enantioselectivity of

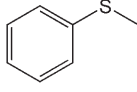
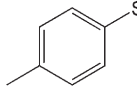
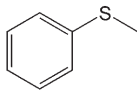
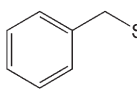
Table 1. Steady-state kinetic parameters of wild-type and M446G PAMO.

No.	Substrate Structure	Wild-type PAMO ^[a,b]			k_{cat} [s^{-1}]	M446G PAMO ^[a]	
		k_{cat} [s^{-1}]	K_{M} [mM]	$k_{\text{cat}}/K_{\text{M}}$ [$\text{M}^{-1} \text{s}^{-1}$]		K_{M} [mM]	$k_{\text{cat}}/K_{\text{M}}$ [$\text{M}^{-1} \text{s}^{-1}$]
<i>Ketones/Aldehydes</i>							
1		3.0	0.08	37500	3.0	1.0	3000
2		2.3	0.1	23000	3.1	0.2	16000
3		-	-	<1	2.9	1.6	1800
4		0.34	2.2	150	-	-	<1
5		1.4	6.9	200	>0.30	>2.5	130
6		>0.06	>1.1	55	>0.02	>5.0	4
<i>Sulfides</i>							
7		>0.12	>2.5	47	>1.3	>2.5	500
8		2.1	0.86	2400	>0.8	>2.0	400
9		0.25	1.5	170	>0.35	>2.0	180
10		1.8	1.6	1100	0.53	2.0	270
11		-	-	<1	>0.11	>1.7	55
<i>Amines</i>							
12		0.03	1.0	32	-	-	<1
13		-	-	<1	>0.30	>20	16
14		-	-	<1	0.30	2.4	130

^[a] Due to solubility limitations, lower limits for k_{cat} and K_{M} are given in some cases.

^[b] Some of the kinetic parameters of wild-type PAMO were adapted from previous studies.^[3d,5]

Table 2. Enantioselective sulfoxidations by wild-type and M446G PAMO.

Substrate No.	Structure	Wild-type PAMO		M446G PAMO	
		Conversion [%]	<i>ee</i> ^[a] [%]	Conversion [%]	<i>ee</i> ^[a] [%]
7		94	41 (R)	>99	93 (R)
8		69	6 (R)	>99	92 (R)
9		94	6 (S)	>99	95 (R)
10		>99	98 (S)	>99	59 (S)

^[a] The predominantly formed enantiomer in parentheses.

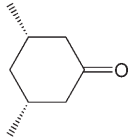
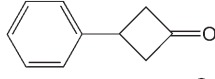
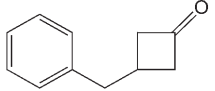
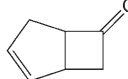
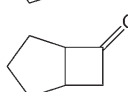
mutant M446G towards this sulfide was found to be lower than that of wild-type PAMO as the *ee* decreased from 98% to 59%. This demonstrates that the M446G mutant nicely complements the catalytic repertoire of the wild-type enzyme. Interestingly, the M446G replacement mimics to some extent the effect of addition of methanol to wild-type PAMO. Recently it was shown that usage of up to 30% methanol is tolerated by PAMO and affects the enantioselectivity.^[4b]

The fact that replacement of M446 can already result in dramatic changes in substrate specificity and enantioselectivity suggests that specific interaction of one or two methanol molecules in the active site may explain the observed solvent effect.

Whole Cell Baeyer–Villiger Oxidation of Cyclic Ketones

To probe whether wild-type and M446G PAMO can be exploited as whole cell biocatalysts, the biooxidation of several prochiral cycloketones was evaluated. Screening experiments were performed in multi-well plastic dishes and conversion and enantioselectivity of microbial reactions were evaluated by chiral GC analysis. It was found that both PAMO variants were effective as whole cell biocatalysts. In general, wild-type PAMO showed higher conversion of ketones but lower enantioselectivity. On the other hand, M446G PAMO oxidized ketones to the corresponding lactones with higher enantioselectivity, but conversions were poor to moderate in all cases. Data included in Table 3 represent a selection of results with striking variations in the biocatalytic performance of wild-type PAMO and the M446G mutant. Interestingly, the M446G mutant was able to oxidize **15** while wild-type PAMO performed best with ketone **17** (Table 3). This demonstrates the subtle changes in substrate specificity as a result of replacing M by G in position 446 of PAMO.

Table 3. Conversions of prochiral cycloketones using wild-type and M446G PAMO expressing cells.

Substrate No.	Structure	Wild-type PAMO		M446G PAMO		
		Conversion ratio lactones ^[a]	<i>ee</i> ^[b] [%]	Conversion ratio lactones ^[a]	<i>ee</i> ^[b] [%]	
15		-	-	4%	28 (-)	
16		23%	5 (+)	traces	10 (-)	
6		35%	11 (-)	12%	65 (-)	
17		65%;	50:50	traces;	70:30	>99/45
18		63%;	90:10	3%;	87:13	97/48

^[a] Ratio of “normal”/“abnormal” lactones.

^[b] Sign of specific rotation in parentheses, while *ee* is given for normal/abnormal lactone.

Conclusions

In recent years it has become popular to employ random mutagenesis approaches (directed evolution) for enzyme redesign. However, such an approach is often not very efficient.^[18] In fact, it appears that for effectively altering the substrate specificity of a biocatalyst one should preferentially target active site or 'first shell' residues.^[18,19] However, such a structure-inspired approach is only feasible when a structure of the targeted biocatalyst is available. For the current study, we exploited the recently determined crystal structure of PAMO. A comparison of the PAMO structure and a homology-built model of CPMO revealed that both active sites are remarkably similar. Only three residues could be identified as significantly different: Q152, L153 and M446. It was postulated that these residues determine to some extent the molecular basis for the two widely different substrate specificities of PAMO and CPMO. While the Q152F/L153G and Q152F/L153G/M446G PAMO mutants were found to be inactive, the M446G mutant shows interesting novel catalytic features while retaining its thermostability. Several new compounds were identified as substrate for this PAMO variant (e.g., indole and benzaldehyde). An altered substrate binding pocket may explain the substantial changes in substrate specificity and enantioselectivity towards sulfides and ketones.

The exact binding mode of substrates in PAMO is uncertain due to the lack of a crystal structure containing a bound substrate. However, several random and directed mutagenesis studies have been performed with PAMO, CHMO and CPMO, providing clues about the residues that form the substrate binding pocket.^[11,13,20] An inventory of all mutations that affect enantioselectivity shows that many targeted residues, including M446, align a pocket at the *re*-face of the flavin cofactor (Figure 2). Future mutagenesis studies can exploit the localization of these hotspots that determine the plasticity of the substrate binding pocket of BVMOs. By this, BVMOs can be created that extend the catalytic potential of the presently available BVMOs and may ultimately combine substrate promiscuity with thermal stability.

Experimental Section

Materials

All chemicals or enzymes were obtained from ACROS Organics, Jülich Fine Chemicals, Roche Applied Sciences and Sigma-Aldrich. Oligonucleotide primers were obtained from Sigma Genosys. DNA sequencing was done at GATC (Konstanz, Germany). The figures have been prepared using the PyMol software (www.pymol.org). The CPMO model

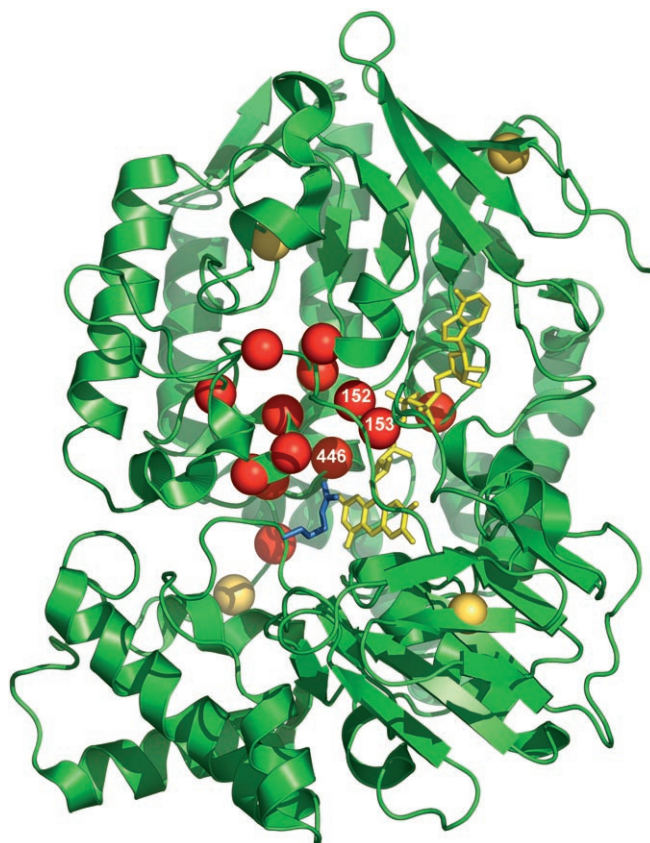


Figure 2. Structure of PAMO in which the FAD cofactor is shown in yellow sticks. The crucial active-site R337 is shown in blue sticks. Observed mutations that effect enantioselectivity of BVMOs are shown by spheres (M446, Q152 and L153 are indicated).^[11,20] Residues that are within 15 Å from the isoalloxazine moiety of the FAD cofactor are in red, more distant residues are in yellow.

has been built using the CPH models server (www.cbs.dtu.dk/services/CPHmodels).

Site-Directed Mutagenesis

For mutagenesis, the previously constructed plasmid pPAMO was used as first template.^[3d] The plasmid contains the *pamo* gene (accession number YP 289549) which is controlled by the P_{BAD} promoter. For preparation of the triple mutant, the single mutated plasmid pPAMO (M446G) was used as template. Mutants were constructed using the QuickChange[®] Site-Directed Mutagenesis Kit of Stratagene with pPAMO as template following the recommendations of the manufacturer. M446 was mutated to G with primer 5'-GCGCTCAGCAACGGCCTGGTCTCTATC-3' and its complementary primer. Q152 and L153 were mutated to F or G with primer 5'-ATGGCCAGCGC**TTTGGCTC**-CGTCCCGCAG-3' and its complementary primer. The mutated nucleotides are shown in bold. The resulting plasmids were transformed into *E. coli* TOP10.

Overexpression and Purification of Wild-Type PAMO and its Mutants

Wild-type PAMO and the mutants were overexpressed in TB medium containing 50 $\mu\text{g mL}^{-1}$ ampicillin and 0.2% L-arabinose at a temperature of 37 °C. Purification of the PAMO mutants was performed as previously described for wild-type PAMO.^[3d]

Steady-State Kinetics

Enzyme concentrations were measured photometrically by monitoring the absorption of the FAD cofactor at 441 nm ($\epsilon_{441\text{nm}} = 12.4 \text{ mM}^{-1} \text{ cm}^{-1}$). The activities of the purified enzymes were determined spectrophotometrically by monitoring the decrease of NADPH in time at 340 nm ($\epsilon_{340\text{nm}} = 6.22 \text{ mM}^{-1} \text{ cm}^{-1}$). Formation of hydrogen peroxide was measured using horseradish peroxidase.^[21] Formation of indigo blue was verified by measuring UV-Vis spectra in 50% acetonitrile which revealed formation of typical absorbance maxima at 287, 337 and 611 nm.^[14c] The reaction mixture (1.0 mL) typically contained 50 mM Tris-HCl, pH 7.5, 100 μM NADPH, 1% (v/v) DMSO, 0.05–1 μM enzyme and 2.0 mM of the substrate of interest (1–14). Kinetic measurements were performed on a Perkin–Elmer Lambda Bio40 spectrophotometer at a temperature of 25 °C. The obtained data were fitted to the Michaelis–Menten equation by non-linear regression analysis (SigmaPlot version 10.0 for Windows).

Enantioselective Oxidations using Purified Enzyme

Enzymatic conversion of substrates 7–10 by wild-type PAMO and mutant M446G were performed at 30 °C in a 2 mL reaction mixture containing 50 mM Tris-HCl, pH 9.0, 100 μM NADPH, 1% (v/v) DMSO, 5 mM glucose 6-phosphate, 5 U glucose 6-phosphate dehydrogenase, 2.5 μM enzyme and 2.5 mM of the substrate of interest. After 90 min the reaction was stopped by extraction with ethylacetate, dried over MgSO_4 and analyzed by gas chromatography. Chiral and achiral GC analyses were performed on a Shimadzu GC17 instrument equipped with an FID and a Chiraldex G-TA column (Alltech, 30 m \times 0.25 mm \times 0.125 mm) or an HP1 column (Agilent, 30 m \times 0.25 mm \times 0.25 mm), respectively. The absolute configuration of the sulfoxides was determined by comparison with the wild-type PAMO-catalyzed enantioselective oxidations.^[5]

Whole Cell Biotransformation in Multi-Well Plates

Each well of 12-well plates was charged with 2 mL of LB medium containing 200 $\mu\text{g mL}^{-1}$ ampicillin and inoculated with 1% v/v of an overnight preculture of TOP10 cells bearing either the wild-type or the M446G PAMO expression plasmids. The plates were incubated at 37 °C and 120 rpm on an orbital shaker. When the appropriate OD_{590} was reached, L-arabinose was added (final concentration of 0.1% w/v) together with the substrates 6, 15–18 (1 mg/12-well format) and shaking continued at 37 °C. After 24 h of cultivation, samples were taken, extracted with ethylacetate supplemented with an internal standard, dried over Na_2SO_4 and analyzed by chiral phase GC (ThermoFinnigan Trace GC 2000 or Focus GC with a BGB 173 or BGB 175

column). The absolute configuration of the lactones was determined by comparison with the currently available literature for CHMO from *Acinetobacter* sp. NCIMB 9871 and CPMO from *Comamonas* sp. strain NCIMB 9872.

Acknowledgements

CERC3 and COST D25/0005/03 are gratefully acknowledged for funding and support.

References

- [1] a) J. D. Stewart, *Biotechnol. Genet. Eng. Rev.* **1997**, *14*, 67–143; b) S. M. Roberts, P. W. H. Wan, *J. Mol. Catal. B* **1998**, *4*, 111–136; c) M. D. Mihovilovic, B. Müller, P. Stanetty, *Eur. J. Org. Chem.* **2002**, *22*, 3711–3730; d) W. J. H. van Berkel, N. M. Kamerbeek, M. W. Fraaije, *J. Biotech.* **2006**, *124*, 670–689.
- [2] a) M. J. Taschner, D. J. Black, *J. Am. Chem. Soc.* **1988**, *110*, 6892–6893; b) V. Alphand, A. Archelas, R. Furstoss, *J. Org. Chem.* **1990**, *55*, 347–350; c) B. Adger, M. T. Bes, G. Grogan, R. McCague, S. P. Moreau, S. M. Roberts, R. Villa, P. W. H. Wan, A. J. Willetts, *Bioorg. Med. Chem.* **1997**, *5*, 253–261; d) J. Lebreton, V. Alphand, R. Furstoss, *Tetrahedron* **1997**, *53*, 145–160; e) C. Mazzini, J. Lebreton, V. Alphand, R. Furstoss, *Tetrahedron Lett.* **1997**, *38*, 1195–1196; f) C. Mazzini, J. Lebreton, V. Alphand, R. Furstoss, *J. Org. Chem.* **1997**, *62*, 5215–5218; g) M. D. Mihovilovic, B. Müller, M. M. Kayser, P. Stanetty, *Synlett* **2002**, *5*, 700–702; h) M. D. Mihovilovic, F. Rudroff, B. Müller, P. Stanetty, *Bioorg. Med. Chem. Lett.* **2003**, *13*, 1479–1482; i) M. D. Mihovilovic, D. A. Bianchi, F. Rudroff, *Chem. Commun.* **2006**, *30*, 3214–3216; j) I. Braun, F. Rudroff, M. D. Mihovilovic, T. Bach, *Angew. Chem. Int. Ed.* **2006**, *45*, 5541–5543.
- [3] a) N. M. Kamerbeek, D. B. Janssen, W. J. H. van Berkel, M. W. Fraaije, *Adv. Synth. Catal.* **2003**, *345*, 667–678; b) M. W. Fraaije, N. M. Kamerbeek, A. J. Heidekamp, R. Fortin, D. B. Janssen, *J. Biol. Chem.* **2004**, *279*, 3354–3360; c) P. C. Brzostowicz, M. S. Blasko, P. E. Rouvière, *Appl. Microbiol. Biotechnol.* **2004**, *58*, 781–789; d) M. W. Fraaije, J. Wu, D. P. H. M. Heuts, E. W. van Hellemond, J. H. Lutje Spelberg, D. B. Janssen, *Appl. Microbiol. Biotechnol.* **2005**, *66*, 393–400; e) H. Iwaki, S. Wang, S. Grosse, H. Bergeron, A. Nagahashi, J. Lertvorachon, J. Yang, Y. Konishi, Y. Hasegawa, P. C. K. Lau, *Appl. Environ. Microbiol.* **2006**, *72*, 2707–2720; f) D. Bonsor, S. F. Butz, J. Solomons, S. Grant, I. J. S. Fairlamb, M. J. Fogg, G. Grogan, *Org. Biomol. Chem.* **2006**, *4*, 1252–1260; g) A. Kirschner, J. Altenbuchner, U. T. Bornscheuer, *Appl. Microbiol. Biotechnol.* **2006**, *75*, 1065–1072; h) T. Kotani, H. Yurimoto, N. Kato, Y. Sakai, *J. Bacteriol.* **2007**, in press.
- [4] a) F. Schulz, F. Leca, F. Hollmann, M. T. Reetz, *Beilstein J. Org. Chem.* **2005**, *1*; b) G. de Gonzalo, G. Ottolina, F. Zambianchi, M. W. Fraaije, G. Carrea, *J. Mol. Catal. B* **2006**, *39*, 91–97.

- [5] G. de Gonzalo, D. E. Torres Pazmiño, G. Ottolina, M. W. Fraaije, G. Carrea, *Tetrahedron: Asymmetry* **2005**, *16*, 3077–3083.
- [6] E. Malito, A. Alfieri, M. W. Fraaije, A. Mattevi, *Proc. Natl. Acad. Sci. USA* **2004**, *101*, 13157–13162.
- [7] N. A. Donoghue, D. B. Norris, P. W. Trudgill, *Eur. J. Biochem.* **1976**, *63*, 175–192.
- [8] M. Griffin, P. W. Trudgill, *Eur. J. Biochem.* **1976**, *63*, 199–209.
- [9] a) M. D. Mihovilovic, F. Rudroff, B. Grötzl, P. Kapitan, R. Snajdrova, J. Rydz, R. Mach, *Angew. Chem. Int. Ed.* **2005**, *44*, 3609–3613; b) M. D. Mihovilovic, F. Rudroff, B. Grötzl, P. Stanetty, *Eur. J. Org. Chem.* **2005**, *5*, 809–816; c) M. D. Mihovilovic, R. Snajdrova, B. Grötzl, *J. Mol. Catal. B* **2006**, *39*, 135–140; d) M. D. Mihovilovic, F. Rudroff, A. Winninger, T. Schneider, F. Schulz, M. T. Reetz, *Org. Lett.* **2006**, *8*, 1221–1224.
- [10] a) F. Zambianchi, P. Pasta, G. Carrea, S. Colonna, N. Gaggero, J. M. Woodley, *Biotechnol. Bioeng.* **2002**, *78*, 489–496; b) H. Iwaki, Y. Hasegawa, S. Wang, M. M. Kayser, P. C. K. Lau, *Appl. Environ. Microbiol.* **2002**, *68*, 5671–5684.
- [11] C. M. Clouthier, M. M. Kayser, M. T. Reetz, *J. Org. Chem.* **2006**, *71*, 8431–8437.
- [12] M. D. Mihovilovic, R. Snajdrova, A. Winninger, F. Rudroff, *Synlett* **2005**, *18*, 2751–2754.
- [13] C. M. Clouthier, M. M. Kayser, *Tetrahedron: Asymmetry* **2006**, *17*, 2649–2653.
- [14] a) B. D. Ensley, B. J. Ratzkin, T. D. Osslund, M. J. Simon, L. P. Wackett, D. T. Gibson, *Science* **1983**, *222*, 167–169; b) N. Mermod, S. Harayama, K. N. Timmis, *Biotechnology* **1986**, *4*, 321–324; c) K. E. O'Connor, A. D. Dobson, S. Hartmans, *Appl. Microbiol. Biotechnol.* **1997**, *63*, 4287–4291; d) H. S. Choi, J. K. Kim, E. H. Cho, Y. C. Kim, J. I. K. S. W. Kim, *Biochem. Biophys. Res. Commun.* **2003**, *306*, 930–936; e) N. Doukyu, K. Toyoda, R. Aono, *Appl. Microbiol. Biotechnol.* **2003**, *60*, 720–725.
- [15] E. E. Snell, *Adv. Enzymol. Relat. Areas Mol. Biol.* **1975**, *42*, 287–333.
- [16] S. Colonna, N. Gaggero, G. Carrea, G. Ottolina, P. Pasta, F. Zambianchi, *Tetrahedron Lett.* **2002**, *43*, 1797–1799.
- [17] J. H. Markgraf, M.-K. Ahn, *J. Am. Chem. Soc.* **1964**, *86*, 2699–2702.
- [18] K. L. Morley, R. J. Kazlauskas, *Trends Biotechnol.* **2005**, *23*, 231–237.
- [19] R. H. H. van den Heuvel, M. W. Fraaije, M. Ferrer, A. Mattevi, W. J. H. van Berkel, *Proc. Natl. Acad. Sci. USA* **2000**, *97*, 9455–9460.
- [20] a) M. T. Reetz, B. Brunner, T. Schneider, F. Schulz, C. M. Clouthier, M. M. Kayser, *Angew. Chem. Int. Ed.* **2004**, *43*, 4075–4078; b) M. T. Reetz, F. Daligault, B. Brunner, H. Hinrichs, A. Deege, *Angew. Chem. Int. Ed.* **2004**, *43*, 4078–4081; c) M. Bocola, F. Schulz, F. Leca, A. Vogel, M. W. Fraaije, M. T. Reetz, *Adv. Synth. Catal.* **2005**, *347*, 979–986.
- [21] Y.-R. Chen, L. J. Deterding, K. B. Tomer, R. P. Mason, *Biochemistry* **2000**, *39*, 4415–4422.